Appendix: Supplementary Information

The supplementary information describes: 1) the steered molecular dynamics simulation method (SI); 2)the extraction of the structural and elastic parameters of the native and the transition states of molecules investigated in this paper (SII); 3) the conformation free energy of a molecule under external force (SIII); 4) an alternative derivation of Eq. 5 (SIV); 5) the determination of the persistence length and contour length per nucleotide for ssDNA (SV); 6) bootstrap analysis to determine fitting errors (SVI); 7) the robustness of convergence of the best-fitting parameters (SVII); 8) analysis of force-dependent PSGL-1/P-selectin disassociation (SVIII) and 9) fitting of Eq. 5 to experimental data of src SH3 domain over different presupposed peptide length in the transition state (SIX).

SI. Molecular dynamics simulations

All-atom molecular dynamics (MD) simulations were performed in Gromacs 5.1.1 [1] with Parmbsc1 force field [2] for DNA and with CHARMM36 force field [3] for proteins. Molecular structures of DNA is built by x3DNA software [4], and the structures of titin I27 domain (PDB: 1tit) [5], monomeric PSGL-1/P-selectin complex (PDB: 1g1s) [6] and src SH3 domain (PDB: 1srl) [7] are public data from protein data bank. All the simulations used explicit water TIP3P [8] with 150 mM NaCl to mimic physiological condition. Simulation boxes were heated to 300 K and then kept at constant temperature and pressure for 200 ps to relax. During steered molecular dynamics simulations, a constant force was applied to the force-bearing residues, therefore the end-to-end distance (extension) fluctuation of the molecules could be analysed. Standard deviation and mean value of extension were calculated from the last 20 ns of simulation.

The transition state of src SH3 is determined by steered MD simulations. A sequence of harmonic traps with same stiffness of 1000 pN/nm and different center separation of 2.1-2.6 nm were applied to the same force-bearing residues as in experiment [9]. With this stretching setup, the force slowly build up between the stretching residues, and the structure has enough time to relax to equilibrium. The force on stretching residues were recorded and concatenated (Fig. S1). Structural transition is indicated by the force drop occured at a trap separation of 2.4 nm. The structure after force drop was regarded as a transition state

of the protein domain during unfolding.

SII. Structural and elastic properties of the native and the transition states of molecules

The contour length of the folded structure in native state or the folded core in transition state of the molecules were estimated based on structures of the molecules (Fig. S2-S4). Molecular dynamics simulations were used to determine the stretching rigidity of typical folded structures. Denoting $b(0)$ and $b(F)$ the folded structure lengths in the absence or presence of force, and assuming Hookean stretching elasticity, we have:

$$b(F) = b(0) + \frac{b(0)}{\gamma} F, \tag{S1}$$

where γ is the stretching rigidity and $\frac{b(0)}{\gamma}$ describes the stretching deformability of the folded structure. Therefore, for a folded structure, γ could be calculated from the linear dependence of $b(F)$ on F.

We calibrated this method for double-stranded DNA (dsDNA), whose stretching rigidity is in the range of $1000 - 3000$ pN, as measured from single-molecule stretching experiments [10–13]. The estimated γ of dsDNA (150 mM NaCl) from our MD simulation is around 1500 pN (Fig. S5), which is consistent with experimentally measured values. Using this approach, we estimated γ for the native state of titin I27 (Fig. S6), as well as the native and transition states of src SH3 (Fig. S7).

SIII. The conformation free energy of a molecule stretched by an external constant force

In general, an external constant force F applied to a molecule in a given state introduces a conformation free energy to the state by:

$$\Phi(x, F) = \int_0^x f(x')dx' - Fx, \tag{S2}$$

where x is the extension of the molecule in this state, and F is the applied force. The external force contributes to a potential energy of $-Fx$. At equilibrium, x is no longer independent from F, since it depends on F through the force-extension curve $x(F)$. Therefore, this energy becomes dependent only on force: $\Phi(x(F), F) = \int_0^{x(F)} f(x')dx' - Fx(F)$, which can be rewritten to a simpler form by Legendre transformation [14, 15]:

$$\Phi(F) = \int_0^F x(F')dF'. \tag{S3}$$

This can be easily seen by the relation (Fig: S8):

$$\int_0^{x_{\rm eq}} f(x')dx' + \int_0^F x(F')dF' = Fx_{\rm eq}. \tag{S4}$$

SIV. Alternative derivation of Eq. 5

Based on the force-dependent free energies of the molecule in both native and transition states that are shown in Eq. 1, $k(F)$ is determined by applying the Arrhenius law $k(F) = k_0 e^{-\beta\Delta\Phi^*(F)}$:

$$k(F) = k_0 e^{-\beta\left(\Phi_{b^*,\gamma^*}(F)+\Phi_{L^*}(F)-\Phi_{b^0,\gamma^0}(F)\right)}. \tag{S5}$$

In the main text, the large force expression Eq. 5 can be derived based on direct asymptotic expansion from Eq. 4. Here we provide an alternative derivation based on large-force expansion of force-extension curves of folded structure and flexible polymer. At large forces ($F \gg k_{\rm B}T/b$ and $F \gg k_{\rm B}T/A$), the force-extension curves of the extensible folded structure and the flexible polymer have very simple asymptotic expressions:

$$\begin{cases} x_{b,\gamma}(F) \approx b(1 - \frac{k_BT}{Fb})(1 + \frac{F}{\gamma}), \\ x_L(F) \approx L(1 - \sqrt{\frac{k_{\rm B}T}{4AF}}). \end{cases} \tag{S6}$$

These expressions are derived based on large force expansion ($F \gg k_{\rm B}T/b$ and $F \gg k_{\rm B}T/A$). The typical sizes of protein domain and the folded core in the transition state are in the order of a few nm; therefore, $k_{\rm B}T/b$ are close to 1 pN. If in the transition state a protein peptide or a ssDNA/ssRNA polymer is produced, due to their very small bending

persistence length of $A \sim 1$ nm, $k_{\mathrm{B}}T/A \sim 5$ pN becomes the predominating factor that imposes a restriction to the lower boundary of force range.

In actual applications, however, the applicable forces do not have to be much greater than 5 pN, since the force-extension curve of a flexible polymer with $A = 0.8$ nm and $L = 5$ nm calculated based on the asymptotic large force expansion differs from the one according to the full Marko-Siggia formula by less than 10% (Fig. S9) at forces above 3 pN.

Based on these large-force asymptotic expressions of the force-extension curves, it is straightforward to show that the force-dependent change in the free energy barrier is:

$$\Delta\Phi^*(F) \approx -\left(\sigma F + \alpha F^2/2 - \eta F^{1/2}\right). \tag{S7}$$

Here $\sigma = L^* + (b^* - b^0) - (\frac{k_{\mathrm{B}}T}{\gamma^*} - \frac{k_{\mathrm{B}}T}{\gamma^0})$, $\alpha = \frac{b^*}{\gamma^*} - \frac{b^0}{\gamma^0}$, and $\eta = L^*\sqrt{\frac{k_{\mathrm{B}}T}{A}}$. Typical values of $\frac{k_{\mathrm{B}}T}{\gamma^0}$ and $\frac{k_{\mathrm{B}}T}{\gamma^*}$ are in the range of 10^{-3} nm - 10^{-2} nm (SI: SI-II); therefore, $\sigma \sim L^* + (b^* - b^0)$. Eq. 5 is obtained by applying the Arrhenius law:

$$k(F) = \tilde{k}_0 e^{\beta\left(\sigma F + \alpha F^2/2 - \eta F^{1/2}\right)}. \tag{S8}$$

SV. Determine the persistence length and contour length per nucleotide for ssDNA

In order to determine the value of persistence length A and the contour length per nucleotide l_r for ssDNA, we measured the force-extension curves of 572 nt ssDNA using magnetic tweezers in 100 mM KCl and 10 mM Tris-HCl (pH 8.0) buffer condition in 23 °C room temperature for 3 independent tethers. Then the experimentally measured ssDNA force-extension curves were fitted by the Marko-Siggia formula (Fig. S11). The best-fitting parameters for persistence length A and the contour length per nucleotide l_r are determined to be $A = 0.714 \pm 0.047$ nm and $l_r = 0.704 \pm 0.015$ nm. The errors are generated by fitting of the force-extension curves from 3 independent tethers.

SVI. Bootstrap analysis to determine fitting errors

In order to test the robustness of fitting of Eq. 5 or Eq. 10 to experimental data, for the molecules studied in our work, we performed 1000 times of fitting with 80% data points that are randomly chosen from the experimentally measured $k(F)$ or $p(F)$ data for

every fitting. We found that all the 1000 sets of the best-fitting parameters are in the reasonable range around the best-fitting parameters that are determined using the whole experimental data. Table S2, Table S3 and Table S4 have shown the averages and the standard deviations of the best-fitting parameters ($\tilde{k}_0$, σ, α, and η) for 1000 times of fitting with the randomly chosen data points, which occupy 80% of the whole experimental data in each fitting. The structural-elastic parameters in the transition state determined based on the native state structure, steered MD simulation, or solved from the best-fitting parameters are also indicated in the tables.

SVII. Robustness of convergence of the best-fitting parameters

We have tested whether the best-fitting values of these parameters in Eq. 5 (σ, α and η) are uniquely determined for a given shape of $k(F)$, by starting from many well-separated different initial values for the fitting of $k(F)$. We used lsqcurvefit function in Matlab to solve the nonlinear curve-fitting (data-fitting) problems in least-squares sense. By starting with different initial points for the fitting, lsqcurvefit may find a local solution that is not particularly close to the global best-fitting parameter values. So if another set of solutions exists that can fit equally well the data, one of the well-separated initial values may lead to a new set of solutions due to the existence of possible local minimums. However, for each of the three molecules tested in the study, we have found that the parameters always converge to the same set regardless of the initial values (Table S5 for I27, Table S6 for sPSGL-1/ sP-selectin, Table S7 for src SH3), which means the best-fitting parameters can be uniquely determined when applying Eq. 5 to fit experimental data of $k(F)$, at least for all the three cases studied in this work.

SVIII. Analysis of force-dependent PSGL-1/P-selectin disassociation

Our analysis about the dissociation kinetics of PSGL-1/P-selectin complex is based on the crystal structure of a PSGL peptide (a.a. 5-18) complexed with a part of P-selectin (a.a. 42 - 198). The value b^0 is measured as the linear distance between P18 of PSGL-1 (a.a. 5-18) and R198 of P-selectin (a.a. 42 - 198). The PSGL-1 peptide interacts with the residues (a.a. 120-155) in P-selectin. Assuming this interaction forms the main binding

interface between PSGL-1 and P-selectin, the complex we chose to do the analysis includes the main interacting interface between the two molecules.

Regarding the influence of the point of force application on both the C-terminus of PSGL-1 and P-selectin, the fitting parameters (σ, α and η) won't change as long as the interacting region is included, since the remaining non-interacting part can be treated as a handle or spacer that does not contribute to the force-dependent transition rate. Correspondingly, the structural parameters L^* and the size difference between the folded core in the transition state and the native state, $b^0 - b^*$, do not change neither. The quantities affected by the change of the force-attaching points are b^0 and b^*, and as a result the apparent stretching rigidity of the native state and the folded core in the transition state is affected. These points are explained with details below.

In the experiments, monomeric PSGL-1 (a.a. 1-279) was coupled through a COOH-terminal biotin to a streptavidin-coated microsphere [16], and the N-terminal region of PSGL-1 interacts with the N-terminal region of P-selectin anchored on the chamber floor at its C-terminal region. Therefore, the sizes of the two molecules are larger than the ones used in our theoretical analysis. As explained by the simple analysis detailed below, this difference should not have a significant influence on the data interpretation, since our analysis includes the main interacting interface.

Fitting Eq. 5 in the main text to the experimental data, the three best-fitting parameters are determined as $\sigma = L^* + b^* - b^0 \sim 0.7$ nm, $\alpha = b^*/\gamma^* - b^0/\gamma^0 \sim -0.005$ nm/pN, and $\eta = L^*\sqrt{k_{\rm B}T/A} \sim 5.8$ nm·pN$^{1/2}$. These three parameters tell the structural-elastic differences between the transition and the native states. Below we show that (σ, α, η) are independent on the size of the proteins constructs used in the experiments, as long as the main binding interface is included.

For convenience, we divide the whole complex of a size b^0 for the native state and b^* for the folded core in the transition state, into two regions: 1) an interacting region that is involved in the formation of the binding interface with a size of $b^0_{\rm it}$ for the native state and $b^*_{\rm it}$ for the folded core in the transition state; 2) the remaining region of a size $b_{\rm c} = b^0 - b^0_{\rm it} = b^* - b^*_{\rm it}$ that is not participated in the transition, and therefore, remains constant during the transition (hereafter we refer it as the constant region) (Fig. S12). Since this constant region is not involved in the interaction, it can be regarded as a handle or spacer that does not contribute to the kinetics.

During transition, a peptide of L^* is produced in the transition state in the interacting region. In addition, the difference of the rigid body size between the native state and the folded core of the transition state, $b^0 - b^*$, is only related to the structural change of the interacting region during transition. Therefore, both L^* and $b^0 - b^*$ are independent on the constant region. As a result, it is easy to see that the fitting parameters σ and η are independent on the constant region.

Next we show that $\alpha = b^*/\gamma^* - b^0/\gamma^0$ is also independent on the constant region. The force-extension curve of a deformable rigid structure with a rod length b can be written as $x(F)/b = g(\beta F b)(1 + F/\gamma) \approx g(\beta F b) + F/\gamma$, where $x(F)$ is the extension, $\beta = (k_{\rm B}T)^{-1}$ and $g(\beta F b) = \coth(\frac{Fb}{k_B T}) - \frac{k_B T}{Fb}$. Taking into account of the typical protein domain size of a few nm, at force above 5 pN, the equation can be more conveniently expressed as (Fig.S13):

$$x(F)/b = g(\beta F b) + F/\gamma. \tag{S9}$$

As mentioned, the native structure or the folded core in the transition state is divided into to a constant region and an interacting region; therefore, its force extension curve can be rewritten as:

$$x^i(F) = b^i g(\beta F b^i) + b^i_{\rm it} F/\gamma^i_{\rm it} + b_{\rm c} F/\gamma_{\rm c}, \tag{S10}$$

where the superscript "i" indicates the states, namely i="0" for the native or i="*" for the folded core in the transition state. Note that the constant region does not dependent on the state index "i".

Denoting θ^i the fraction of the folded structure size of the interacting region relative to the total size, $b^i_{\rm it} = \theta^i b^i$ and therefore $b_{\rm c} = (1 - \theta^i) b^i$. It is easy to see that the expression (Eq. S10) can be rewritten as:

$$x^i(F) = b^i g(\beta F b^i) + b^i F/\tilde{\gamma}^i, \tag{S11}$$

where the effective stretching rigidity is

$$\tilde{\gamma}^i = \gamma^i_{\rm it}/[\theta^i + (1 - \theta^i)\gamma^i_{\rm it}/\gamma_{\rm c}]. \tag{S12}$$

Based on these relations, one can show that: $b^i/\tilde{\gamma}^i = b^i_{\rm it}/\gamma^i_{\rm it} + b_{\rm c}/\gamma_{\rm c}$. Therefore, we have:

$$\alpha = b^*/\tilde{\gamma}^* - b^0/\tilde{\gamma}^0 = b^*_{\rm it}/\gamma^*_{\rm it} - b^0_{\rm it}/\gamma^0_{\rm it}. \tag{S13}$$

As such, the parameter α only depends on the differential deformability of the binding interface between the transition state and native state, independent on the rest constant domains.

The above analysis shows that the three model parameters σ, α and η are associated with the intrinsic nature of the binding interface, independent on the rest constant regions of the proteins. It implies that L^* and $(b^0 - b^*)$ are constant. In experiments and in theoretical analysis, the size of the construct b^0 can be chosen; however, this choice does not affect (σ, α, η) and (L^*, $(b^0 - b^*)$). It only affects the apparent stretching rigidity as shown in Eq. S12.

Besides, the assumption of $\gamma^0 = \gamma^*$ not only be valid for our interpretation for the experimental data of P-selectin/PSGL-1 dissociation in the main text based on the truncated P-selectin/PSGL-1 peptide structure, but also be valid for the analysis with the complete P-selectin/PSGL-1 complex. As shown by Eq. S12, when the size of the interacting region is much smaller than the total size (i.e., $\theta << 1$), the apparent stretching rigidity converges to $\gamma_{\rm c}$ regardless of whether the molecule is in the native or the transition state. Based on the structure (Fig. S3), the size of interacting region is less than 1/5 of the total size. On this basis we set $\gamma^0 = \gamma^*$. Note here γ is the apparent stretching rigidity of the molecule, instead of the stretching rigidity of the interacting region. If a complete PSGL-1 molecule is used, the fraction θ will be even smaller; therefore, based on the reasons detailed above, we can reasonably assume that the approximation of $\gamma^0 = \gamma^*$ still holds.

SIX. Fitting of Eq. 5 to experimental data of src SH3

In the fitting of Eq.5 to the $k(F)$ data of src SH3, $\eta < 4.3$ nm·pN$^{1/2}$ is needed to ensure a positive b^*. By restricting the number of residues of the flexible peptide in the transition state of src SH3, good quality of fitting can be obtained (Fig. S14), which suggests that the peptide length is not a key factor for the $k(F)$ profile. At each peptide length, the best-fitting parameters predict $\alpha > 0$ and $\gamma^* \ll \gamma^0$, indicating that a much softer folded core in the transition state than that of the native state is the predominant factor of $k(F)$

(Table S8). Previous study estimated a small transition distance ~ 0.45 nm in the force range of $15 - 25$ pN [9], suggesting insignificant fraction of peptide in the transition state. Otherwise, considering $0.22 - 0.28$ nm per residue of typical peptide in $15 - 25$ pN force range [17], one would expect a significantly larger transition distance if a long peptide (> 3 a.a) is produced in the transition state.

[1] M. J. Abraham, T. Murtola, R. Schulz, S. Páll, J. C. Smith, B. Hess, and E. Lindahl, SoftwareX **1**, 19 (2015).

[2] I. Ivani, P. D. Dans, A. Noy, A. Pérez, I. Faustino, A. Hospital, J. Walther, P. Andrio, R. Goñi, A. Balaceanu, *et al.*, Nature methods **13**, 55 (2016).

[3] R. B. Best, X. Zhu, J. Shim, P. E. Lopes, J. Mittal, M. Feig, and A. D. MacKerell Jr, Journal of chemical theory and computation **8**, 3257 (2012).

[4] X.-J. Lu and W. K. Olson, Nucleic acids research **31**, 5108 (2003).

[5] S. Improta, A. S. Politou, and A. Pastore, Structure **4**, 323 (1996).

[6] W. S. Somers, J. Tang, G. D. Shaw, and R. T. Camphausen, Cell **103**, 467 (2000).

[7] H. Yu, M. K. Rosen, and S. L. Schreiber, FEBS letters **324**, 87 (1993).

[8] W. L. Jorgensen, J. Chandrasekhar, J. D. Madura, R. W. Impey, and M. L. Klein, The Journal of chemical physics **79**, 926 (1983).

[9] B. Jagannathan, P. J. Elms, C. Bustamante, and S. Marqusee, Proc. Natl. Acad. Sci. U.S.A. **109**, 17820 (2012).

[10] C. Bustamante, S. B. Smith, J. Liphardt, and D. Smith, Current opinion in structural biology **10**, 279 (2000).

[11] J. Marko and E. Siggia, Macromolecules **28**, 8759 (1995).

[12] H. Fu, H. Chen, X. Zhang, Y. Qu, J. F. Marko, and J. Yan, Nucleic Acids Res. **39**, 3473 (2011).

[13] X. Zhang, H. Chen, S. Le, I. Rouzina, P. S. Doyle, and J. Yan, Proc. Natl. Acad. Sci. U.S.A. **110**, 3865 (2013).

[14] S. Cocco, J. Yan, J.-F. Léger, D. Chatenay, and J. F. Marko, Physical Review E **70**, 011910 (2004).

[15] I. Rouzina and V. A. Bloomfield, Biophysical journal **80**, 882 (2001).

[16] T. Yago, A. Leppänen, H. Qiu, W. D. Marcus, M. U. Nollert, C. Zhu, R. D. Cummings, and R. P. McEver, J Cell Biol **158**, 787 (2002).

[17] R. S. Winardhi, Q. Tang, J. Chen, M. Yao, and J. Yan, Biophysical Journal **111**, 2349 (2016).

[18] H. Lu, B. Isralewitz, A. Krammer, V. Vogel, and K. Schulten, Biophys. J. **75**, 662 (1998).

[19] H. Lu and K. Schulten, Chem. Phys. **247**, 141 (1999).

[20] R. B. Best, S. B. Fowler, J. L. Herrera, A. Steward, E. Paci, and J. Clarke, J. Mol. Biol. **330**, 867 (2003).

[21] P. M. Williams, S. B. Fowler, R. B. Best, J. L. Toca-Herrera, K. A. Scott, A. Steward, and J. Clarke, Nature **422**, 446 (2003).

Supplementary tables

TABLE S1. γ (pN) for different structures

dsDNA	I27	SH3 native	SH3 transition
1500	1900	2900	86

TABLE S2. Parameters for I27 by fitting Eq. 5 to 1000 sets of 80% data points

	Best-fitting parameters				Structural-elastic parameters		
	$\tilde{k}_0$ (s^{-1})	σ (nm)	α (nm/pN)	η (nm·$pN^{1/2}$)	L^* (nm)	b^* (nm)	γ^* (pN)
Average	0.026	1.014	0.003	10.023	4.4	0.9	179
Standard deviation	0.014	0.243	0.003	1.542	0.7	0.4	41

TABLE S3. Parameters for PSGL-1/P-selectin complex by fitting Eq. 5 to 1000 sets of 80% data points

	Best-fitting parameters				Structural-elastic parameters		
	$\tilde{k}_0$ (s^{-1})	σ (nm)	α (nm/pN)	η (nm·$pN^{1/2}$)	L^* (nm)	b^* (nm)	γ^0=γ^* (pN)
Average	58.498	0.727	-0.005	5.752	2.5	5.5	379
Standard deviation	27.083	0.162	0.001	1.275	0.6	0.4	48

TABLE S4. Parameters for src SH3 by fitting Eq. 5 to 1000 sets of 80% data points

	Best-fitting parameters			Structural-elastic parameters	
	$\tilde{k}_0$ (s^{-1})	σ (nm)	α (nm/pN)	b^* (nm)	γ^* (pN)
Average	0.045	-0.475	0.050	1.4	29
Standard deviation	0.043	0.249	0.009	0.2	9

TABLE S5. Best-fitting parameters for I27 with different initial values

	Initial values				Best-fitting values			
Case	$\tilde{k}_0$ (s^{-1})	σ (nm)	α (nm/pN)	η (nm·$pN^{1/2}$)	$\tilde{k}_0$ (s^{-1})	σ (nm)	α (nm/pN)	η (nm·$pN^{1/2}$)
1	0.01	-10	-10	0	0.026	1.099	0.002	10.519
2	0.01	-10	-10	5	0.026	1.099	0.002	10.519
3	0.01	-10	-10	10	0.026	1.099	0.002	10.519
4	0.01	0	0	5	0.026	1.099	0.002	10.519
5	0.01	0	0	10	0.026	1.099	0.002	10.519
6	0.01	10	0	5	0.026	1.099	0.002	10.519
7	0.01	0	10	5	0.026	1.099	0.002	10.519
8	1	0	0	10	0.026	1.099	0.002	10.519
9	0.00001	0	0	10	0.026	1.099	0.002	10.519
10	1	10	10	10	0.026	1.099	0.002	10.519

TABLE S6. Best-fitting parameters for PSGL-1/P-selectin complex with different initial values

	Initial values				Best-fitting values			
Case	$\tilde{k}_0$ (s^{-1})	σ (nm)	α (nm/pN)	η (nm·$pN^{1/2}$)	$\tilde{k}_0$ (s^{-1})	σ (nm)	α (nm/pN)	η (nm·$pN^{1/2}$)
1	1	0	0	0	51.786	0.723	-0.005	5.760
2	1	0	0	5	51.786	0.723	-0.005	5.760
3	1	0	0	10	51.786	0.723	-0.005	5.760
4	1	5	0	0	51.786	0.723	-0.005	5.760
5	1	10	0	0	51.786	0.723	-0.005	5.760
6	1	10	10	10	51.786	0.723	-0.005	5.760
7	1	0	-5	5	51.786	0.723	-0.005	5.760
8	1	0	-10	5	51.786	0.723	-0.005	5.760
9	10	0	0	5	51.786	0.723	-0.005	5.760
10	100	0	0	5	51.786	0.723	-0.005	5.760

TABLE S7. Best-fitting parameters for src SH3 with different initial values

	Initial values			Best-fitting values		
Case	$\tilde{k}_0$ (s^{-1})	σ (nm)	α (nm/pN)	$\tilde{k}_0$ (s^{-1})	σ (nm)	α (nm/pN)
1	0.1	0	0	0.030	-0.441	0.049
2	0.1	0	10	0.030	-0.441	0.049
3	0.1	0	100	0.030	-0.441	0.049
4	0.1	10	-10	0.030	-0.441	0.049
5	0.1	10	-100	0.030	-0.441	0.049
6	0.1	-10	10	0.030	-0.441	0.049
7	0.1	-100	10	0.030	-0.441	0.049
8	10	10	10	0.030	-0.441	0.049
9	100	10	10	0.030	-0.441	0.049
10	100	100	100	0.030	-0.441	0.049

TABLE S8. Fitting parameters for src SH3

n^*	L^* (nm)	η (nm·$pN^{1/2}$)	σ (nm)	α (nm/pN)	γ^* (pN)
1	0.38	0.86	-0.317	0.048	25
2	0.76	1.7	-0.196	0.046	20
3	1.14	2.6	-0.066	0.044	16
4	1.52	3.4	0.049	0.043	10
5	1.90	4.3	0.179	0.042	4

n^* is the number of residues assumed for the peptide length in the transition state of src SH3. L^* is the contour length of the flexible polymer, which is determined based on $L^* = n^* l_{\mathrm{r}}$ and $l_{\mathrm{r}} \sim 0.38$ nm for peptide chain. The value of η is restricted by $\eta = L^* \sqrt{\frac{k_{\mathrm{B}}T}{A}}$ in the fitting of Eq. 2 to the experimental data of src SH3 for each peptide length. σ and α are the besting fitting values. Based on the structure of the native state and using steered MD simulation, the structural-elastic parameters of the native state are determined to be $b^0 \sim 1.90$ nm and $\gamma^0 \sim 2900$ pN (SII). From these parameters, the value of γ^* was solved for each presupposed peptide length. The goodness-of-fit is evaluated by R-square ~ 0.992 for all the fittings.

Supplementary figures

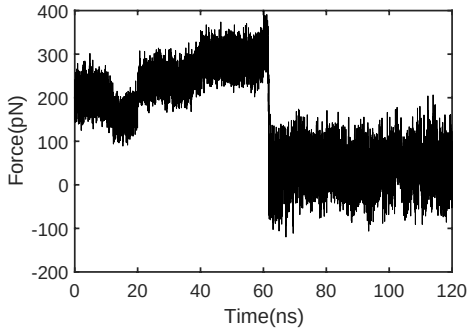

FIG. S1. **Force applied on src SH3 domain during steered MD simulation.** Forces from a sequence of simulation (20 ns each) with increasing harmonic trap separation from 2.1nm-2.6nm were concatenated. At beginning, stepwised increase in force was observed as trap separation increased. As the trap separation increased to 2.4nm, the force initially increased at the begining of simulation and then suddenly dropped off, indicating a structural reorganization in the protein domain. We reason this state after the abrupt force drop could be the transition state because it is still an overall folded structure and it has a structural-elastic difference from the native state. In this state, no significant amount of peptide is produced. The force drop was followed by a much weaker dependence of force on trap separation as the separation continued to increase, indicating a very different structure produced under stretching. Thus the structure after force drop was characterised as a transition state.

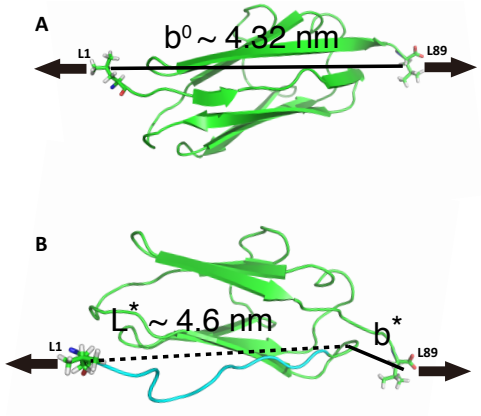

FIG. S2. **The structure of titin I27 domain in the native state and the transition state.** (A) The native state of I27 is a folded structure with $b^0 = 4.32$ nm. (B) The transition state of I27 is composed of a peptide of 13 residues [18–21] under force and a folded core with a relaxed length of $b^* = 0.8$ nm. The two force attaching points L1 and L89 residues are indicated.

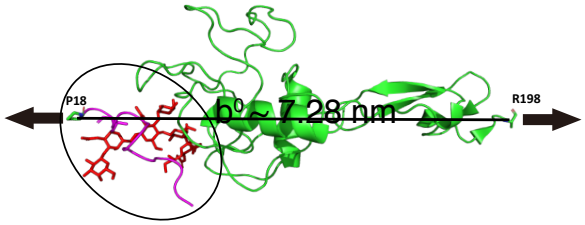

FIG. S3. **The structure of monomeric PSGL-1/ P-selectin complex in native state.** The crystal structure of the binding interface of monomeric PSGL-1 - P-selectin complex includes residues Y5-P18 for PSGL-1 and residues W42-R198 for P-selectin (1g1s). The protein complex has a folded structure length of $b^0 = 7.28$ nm. It contains a SLe^x sugar chain (red) covalently linked to PSGL-1 (magenta) that binds to P-selectin (green). The interacting region (shown within the black circle) occupies a small fraction of the whole complex.

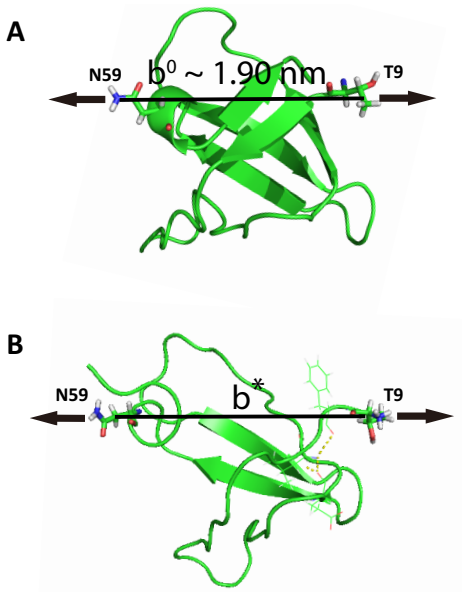

FIG. S4. **The structure of src SH3 in native state and transition state under force.** For src SH3, two point mutations were made at the (A7C) and (N59C), to enable force attaching to these two sites in the experiment [9]. The crystal structure of src SH3 (PDB: 1srl) only contains residues from T9 to S64. In our calculation, b^0 is estimated based on the linear distance between T9 and N59. In the MD simulation, force was also applied to T9 and N59. Since the residues 7 and 9 only differ by two amino acids, the difference should not influence the results significantly. (A) In the native state, the distance between force-bearing residues is 1.90 nm, thus it is regarded as a folded structure with a relaxed length of $b^0 = 1.90$ nm. (B) A snapshot of the transition state produced by sequential stretching by harmonic traps (SI: Sec I). The hydrogen bonds in N-terminal remains (as shown in yellow dashed lines, key residues involved are shown in line representation), while the C-terminal peptide peels off, which is not under force, so the released peptide under force is negligible.

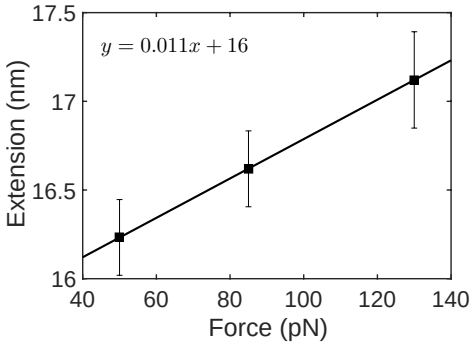

FIG. S5. **Stretching rigidity of dsDNA molecule.** Extension of 50 bp dsDNA was measured at constant forces (squares in the figure show the average value of extension and vertical error bars indicate the standard deviation). The simulations run for 50 ns, during which no structural transition occurs, so the extensions were a pure elastic response. The fitting parameter of the slope s is determined to be (with 95% confidence bounds): $s = 0.011$ $(0.011, 0.011)$ nm/pN. Based on the well-known B-form DNA contour length ~ 0.34 nm per basepair, the value of b is determined as $b \sim 0.34 \times 50 = 17$ nm. As a result, the stretching rigidity of dsDNA molecule is estimated to be $\gamma \sim 1500$ pN.

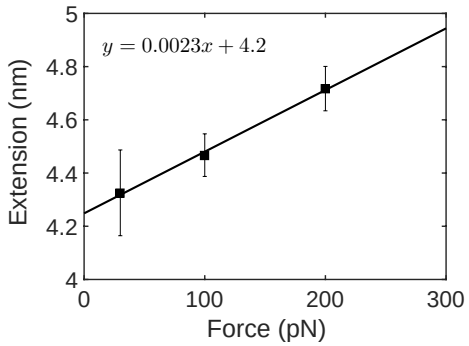

FIG. S6. **Stretching rigidity of titin I27 domain in native state.** Extension of titin I27 domain in the native state was measured at constant forces (squares in the figure show the average value of extension and vertical error bars indicate the standard deviation). The simulations run for 50 ns, during which no structural transition occurs, so the extensions were a pure elastic response. The fitting parameter of the slope s is determined to be (with 95% confidence bounds): $s = 0.0023$ $(0.0006, 0.0040)$ nm/pN. According to the value of $b \sim 4.3$ nm, which is obtained based on the structure of I27 in native state, the stretching rigidity of folded titin I27 domain is estimated to be $\gamma \sim 1900$ pN.

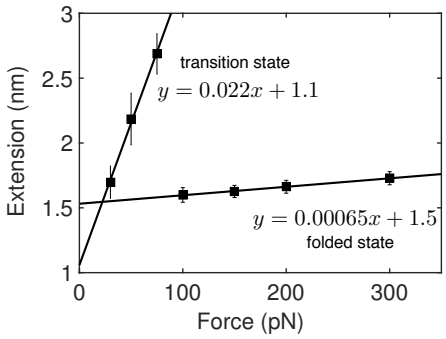

FIG. S7. **Stretching rigidity of src SH3 domain in native state and transition state.** Extension of src SH3 domain in the native and transition states were measured at constant forces (squares in the figure show the average value of extension and vertical error bars indicate the standard deviation). The simulations run for 50 ns, during which no structural transition occurs, so the extensions were a pure elastic response. For the native state, the fitting parameter of the slope s is determined to be (with 95% confidence bounds): $s = 0.00065$ $(0.00057, 0.00073)$ nm/pN. According to the value of $b \sim 1.90$ nm, which is obtained based on the structure of src SH3 in native state, the stretching rigidity of folded src SH3 is estimated to be $\gamma \sim 2900$ pN. Similarly, the slope s for transition state is determined to be $s = 0.022$ $(0.007, 0.037)$ nm/pN. Since the folded core of the transition state maintains the overall structure as in the native state, the value of b is also estimated to be $b \sim 1.90$ nm for the transition state, from which the stretching rigidity of the transition state of src SH3 is calculated to be $\gamma \sim 86$ pN.

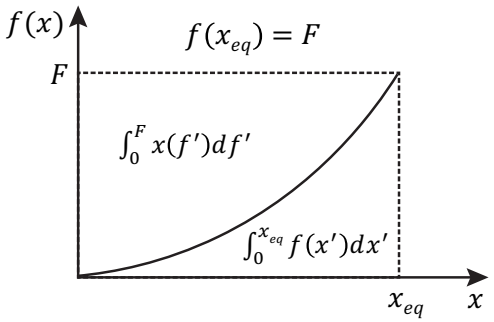

FIG. S8. **The conformation free energy of a molecule under external force.** At equilibrium, the conformation free energy of a molecule under force $\Phi(x(F), F) = \int_0^{x(F)} f(x')dx' - Fx(F)$ equals $\Phi(F) = \int_0^F x(F')dF'$.

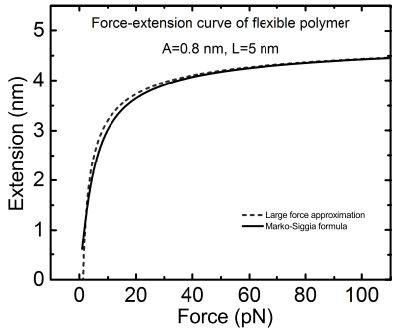

FIG. S9. **Force-extension curves of flexible polymer.** The force-extension curve of a flexible polymer with $A = 0.8$ nm and $L = 5$ nm calculated based on the asymptotic large force expansion (dash line) differs from the one from the full Marko-Siggia formula (solid line) by less than 10%.

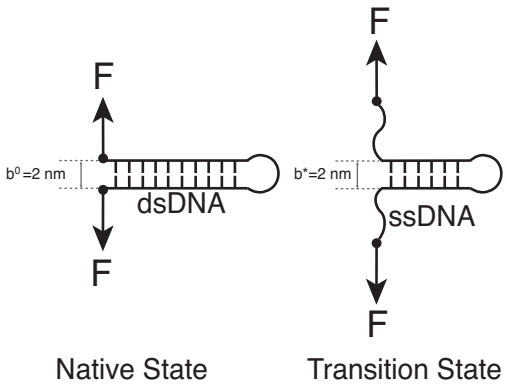

FIG. S10. **The native and transition state of DNA hairpin unzipping.** The rigid body lengths for both the native and the transition state are the same, $b = b^* \sim 2$ nm, which is the diameter of a B-form dsDNA.

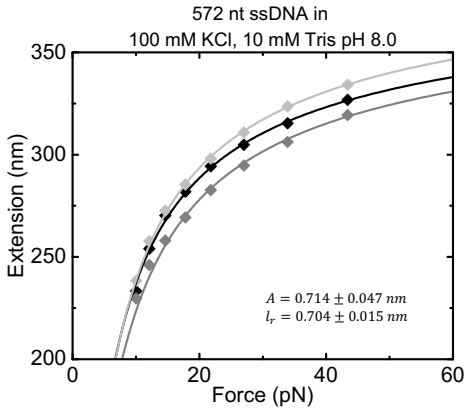

FIG. S11. **The determination of the persistence length and the contour length per nucleotide for ssDNA.**The experimentally measured force-extension curves of 572nt ssDNA using magnetic tweezers from 3 different tethers were fitted by Marko-Sigga formula. The best-fitting parameters of the persistence length A and the contour length per nucleotide l_r are indicated.

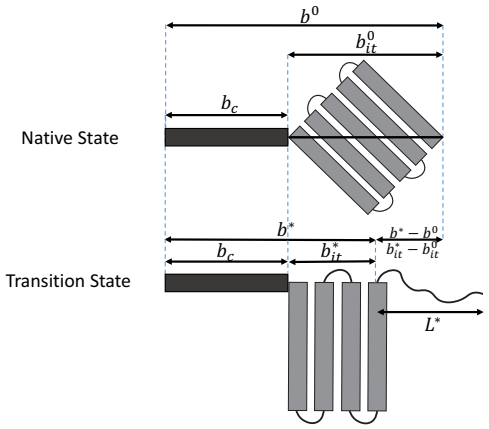

FIG. S12. **The schematics of the interacting region and the constant region in the native state and the transition state.** $b_{\rm it}^0$ and $b_{\rm it}^*$ are the interacting region of the native state and the folded core in the transition state, respectively. $b_{\rm c}$ is the constant region which is not involved during transition. From the sketch, it is clear to see that $b^0 - b^*$ always equals $b_{\rm it}^0 - b_{\rm it}^*$, and it is independent on the choice of b^0.

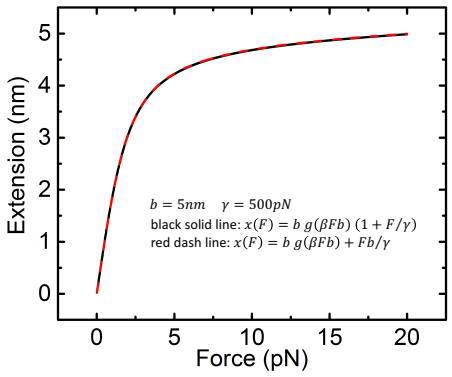

FIG. S13. **The force-extension curves of a deformable rigid body.** With the parameters of $b = 5$ nm and $\gamma = 500$ pN, the force-extension curves expressed by $x(F)/b = g(\beta F b)(1 + F/\gamma)$ and $x(F)/b = g(\beta F b) + F/\gamma$ are almost the same.

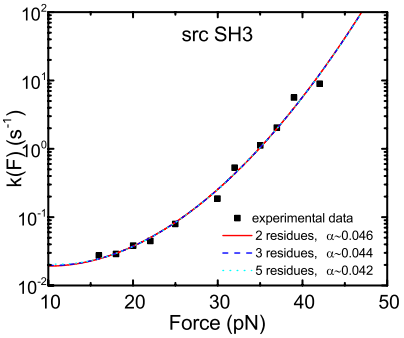

FIG. S14. **Fitting of Eq. 5 to experimental data of src SH3.** By restricting the number of residues of the flexible peptide in the transition state of src SH3, good quality of fitting can be obtained. The figure shows the fitting curves of experimental data for src SH3 domain when the number of peptide residue is presupposed to be 2, 3 and 5. The goodness-of-fit is evaluated by R-square ~ 0.992 for all the fittings.